

# The $\overline{\text{P}}\text{ANDA}$ Detector at FAIR

**W Ikegami Andersson**  
**on behalf of the  $\overline{\text{P}}\text{ANDA}$  collaboration**

Department of Physics and Astronomy, Uppsala University, Box 516, S-751 20 Uppsala,  
Sweden

E-mail: `walter.ikegami.andersson@physics.uu.se`

**Abstract.** The future  $\overline{\text{P}}\text{ANDA}$  detector at FAIR is a state-of-the-art internal target detector designed for strong interaction studies. By utilizing an antiproton beam, a rich and unique physics programme has been realized. The  $\overline{\text{P}}\text{ANDA}$  experiment, as well as feasibility studies for hyperon and charmonium physics, are discussed.

## 1. Introduction

The accepted theory of the strong interaction is Quantum Chromodynamics (QCD). It describes the properties of quarks and their interactions through gluons, the force mediator of the strong interaction. QCD is very successful in predicting processes at high energies where the coupling constant  $\alpha_s$  is small and perturbation theory is applicable. However, at low energies, the theory becomes strongly coupled as  $\alpha_s$  grows large. In this non-perturbative regime, it is still hard to make predictions from first principles. This give rise to many questions: Are there effective degrees of freedom which can systematically describe resonances and bound states? Where are the exotic resonances and bound states predicted by QCD? The future  $\overline{\text{P}}\text{ANDA}$  detector is the ideal experiment to answer these questions. A major part of the  $\overline{\text{P}}\text{ANDA}$  physics programme is to collect large statistics and high-quality data and test QCD in the non-perturbative regime. In the following sections, the  $\overline{\text{P}}\text{ANDA}$  experiment is introduced and three aspects of its physics programme will be highlighted.

## 2. The $\overline{\text{P}}\text{ANDA}$ experiment

The Facility for Antiproton and Ion Research (FAIR) is an accelerator facility under construction at GSI (Gesellschaft für Schwerionenforschung) in Darmstadt, Germany. The  $\overline{\text{P}}\text{ANDA}$  detector will be situated in the high-energy storage ring (HESR) at FAIR. HESR will provide an antiproton beam with momenta from 1.5 up to 15 GeV/c, which corresponds to center-of-mass energies between 2.0 and 5.5 GeV/c<sup>2</sup>. HESR will support two modes of operation, high resolution mode and high luminosity mode. In the high luminosity mode, a luminosity of  $\mathcal{L} \approx 2 \times 10^{32} \text{ cm}^{-2}\text{s}^{-1}$  will be provided. Stochastic cooling will be used to achieve a beam momentum resolution of  $\Delta p/p = 10^{-4}$ . The high resolution mode will provide a luminosity of  $\mathcal{L} \approx 2 \times 10^{31} \text{ cm}^{-2}\text{s}^{-1}$  and a beam momentum resolution of  $\Delta p/p = 5 \times 10^{-5}$  with the use of stochastic cooling. During the startup phase, the accumulator preceding HESR will not be present. At this stage, HESR will provide a luminosity of  $\mathcal{L} \approx 10^{31} \text{ cm}^{-2}\text{s}^{-1}$ .

The  $\bar{\text{P}}\text{ANDA}$  detector, shown in Figure 1, consists of a target spectrometer (TS) and a forward spectrometer (FS) which provide almost full coverage of the solid angle. The target will be either a cluster jet or frozen hydrogen pellets. Thin foils will be used for  $\bar{p}A$  studies. The interaction point is surrounded by the Micro Vertex Detector (MVD) which has a spatial resolution of  $50\ \mu\text{m}$  in  $x$ - and  $y$ -direction and  $100\ \mu\text{m}$  in the  $z$ -direction. In addition to the MVD, the Straw Tube Tracker (STT) and Gas Electron Multiplier (GEM) stations will be used for tracking charged particles ( $\Delta p_t/p_t = 1.2\%$ ). Photons will be reconstructed with the Electromagnetic Calorimeter (EMC). The EMC consists of a barrel, a forward endcap and backward endcap and is made up of 17200  $\text{PbWO}_4$  crystals. Particle identification of pions, kaons and protons will utilise information from a Time-of-Flight (ToF) and a barrel Detection of Internally Reflected Cherenkov light (DIRC) detector. A solenoid magnet will provide a homogeneous magnetic field up to 2T in the beam direction. Outside of the solenoid, muon chambers are placed for identification of muons.

The FS covers polar angles below  $10^\circ$  horizontally and  $5^\circ$  vertically. Charged particles will be detected using the Forward Tracking System (FTS), which consists of multiple straw tube layers, in conjunction with a dipole magnet. The Forward Time-of-Flight (FToF) and the aerogel Ring Imaging Cherenkov Counter (FRICH) detectors will provide particle identification. Calorimetry is performed with a Shashlyk-type Calorimeter (FSC). Behind the FSC, the Muon Range System is placed for identification of muons. A detailed description of the  $\bar{\text{P}}\text{ANDA}$  detector is given in Ref. [1]. All simulation studies in the following sections assume the full detector setup.

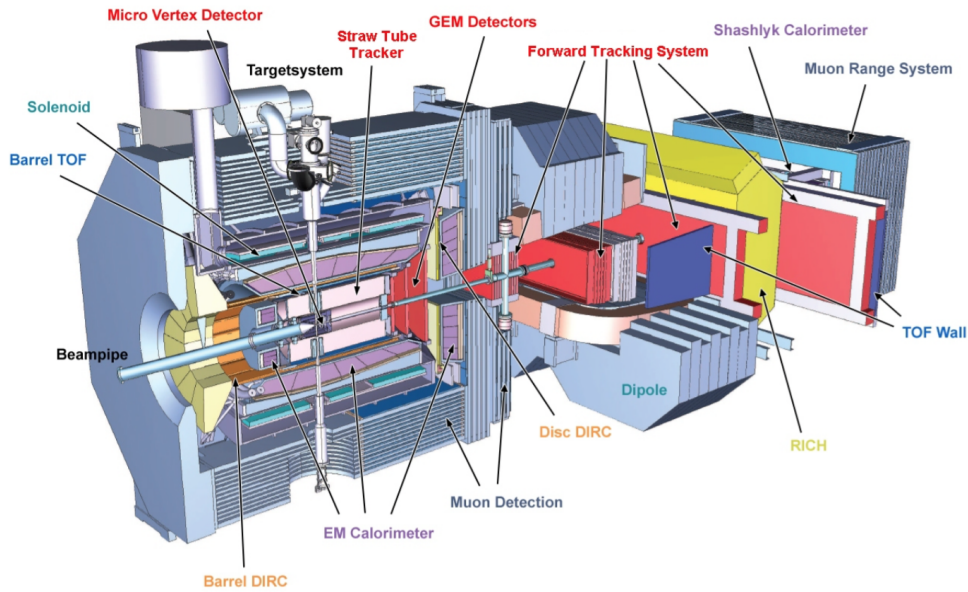


**Figure 1.** The  $\bar{\text{P}}\text{ANDA}$  detector setup.

### 3. Charmonium spectroscopy

One open question within the Standard Model is the existence of exotic states such as glueballs, hybrids and multiquark states, which are expected by QCD. From experiment candidates for exotics exist, but none of them has been identified unambiguously. The field of charmonium spectroscopy is an exciting field with many new states discovered in the past 13 years. So far, all of the predicted charmonium states with masses below the  $D\bar{D}$  threshold have been observed with properties in line with predictions. However, the situation above the  $D\bar{D}$  threshold is less clear. Many predicted states have not yet been observed. On the other hand, unexpected states

have been measured by various experiments *e.g.* BaBar, Belle, BESIII. The properties of these states are not in agreement with the Quark Model expectations of the charmonium spectra.

One of the most intriguing state is the  $X(3872)$ . It was first observed by Belle in 2003 in the decay  $X(3872) \rightarrow J/\psi\pi^+\pi^-$  [2] and has since then been confirmed by several other experiments [3, 4, 5, 6, 7]. Its quantum numbers,  $J^{PC} = 1^{++}$ , have been determined by LHCb [8]. This makes the  $X(3872)$  a candidate for the excited  $\chi_{C1}(2P)$  state. However, since its mass is very close to the  $D^{*0}\bar{D}^0$  threshold, it could also be a loosely bound  $D^{*0}\bar{D}^0$  molecule or a virtual scattering state. In the case of a molecule or virtual state, the line-shape of the  $X(3872)$  state is expected to be different from a Breit-Wigner [9, 10]. Thus, a precise measurement of the line-shape is the key to identify its nature. The upper limit for the width of the  $X(3872)$  is  $\Gamma < 1.2$  MeV, which was measured by Belle [11]. A more precise measurement of the width is unfeasible with currently running experiments as they are limited by their detector resolutions. By producing the  $X(3872)$  in formation reactions  $A+B \rightarrow X(3872)$ , the width can be measured with higher precision by the means of a resonance scan. However, no current experiment can produce the quantum numbers  $J^{PC} = 1^{++}$  in leading order.  $\bar{P}$ ANDA is the ideal experiment as  $\bar{p}p$  annihilation can produce all non-exotic  $J^{PC}$  quantum numbers directly.

To illustrate the potential of measuring the width of the  $X(3872)$ , a Monte Carlo study has been performed. The process  $X(3872) \rightarrow J/\psi\pi^+\pi^- \rightarrow l^+l^-\pi^+\pi^-$  along with relevant background channels were generated at 40 scan points around the nominal center-of-mass energy with a step size of  $dE \approx 70$  keV. A MC sample equivalent to two days of beam time was simulated for each scan point which corresponds to a total of 80 days of beam time. Both the high luminosity mode and the high resolution mode with the startup luminosity have been tested. In order to get an impression of the expected sensitivity and bias of a width measurement, the toy MC experiment was repeated  $N_{\text{MC}} = 300$  times. A Breit-Wigner distribution was fitted to the scan points in the energy dependent yield distribution. The difference between the extracted width  $\Gamma_{\text{meas}}$  and the input width  $\Gamma_0$  in each simulation was noted. The sensitivity and bias are based on the mean value and the root-mean-square of the  $\Gamma_{\text{meas}} - \Gamma_0$  distribution and are defined as

$$\frac{\Delta\Gamma_{\text{meas}}}{\bar{\Gamma}_{\text{meas}}} = \frac{\text{RMS}}{\text{Mean} + \Gamma_0} \pm \frac{\text{RMS}}{\text{Mean} + \Gamma_0} \sqrt{\frac{1}{2(N_{\text{MC}} - 1)} + \frac{\text{RMS}^2}{N_{\text{MC}} \cdot (\text{Mean} + \Gamma_0)^2}} \quad (1)$$

$$\frac{\bar{\Gamma}_{\text{meas}} - \Gamma_0}{\Gamma_0} = \frac{\text{RMS}}{\Gamma_0} \pm \frac{\text{RMS}}{\Gamma_0\sqrt{N_{\text{MC}}}}. \quad (2)$$

The sensitivity and bias are calculated for the following values of the input width  $\Gamma_0 \in [50, 70, 100, 130, 180, 250, 500]$  keV. See Figure 2.

The sensitivity is expected to be better than 20% for input widths  $\Gamma_0 > 90$  keV for high luminosity mode and  $\Gamma_0 > 120$  keV for high resolution mode with the startup luminosity. Furthermore, the experimental bias is negligible within errors. A similar study where a  $\bar{D}D^*$  molecule picture is assumed has also been performed. More details about the study, including a sensitivity test of a molecule description, can be found in Ref. [12].

#### 4. Baryon spectroscopy

Baryon spectroscopy is another field that explores the dynamics of quarks and gluons confined into hadrons. Baryon spectroscopy has played an integral part in the development of QCD. One of the great successes of baryon spectroscopy is the formulation of the quark model. Starting in the 1950s, many new particles were discovered and soon it became clear that these particles could not all be elementary. Among the newly discovered particles, some seemed to match the representation of a SU(3) symmetry. The Eightfold Way was introduced in 1962 to organize spin- $\frac{1}{2}$  baryons into an octet and spin- $\frac{3}{2}$  baryons into a decuplet. In particular, the spin- $\frac{3}{2}$

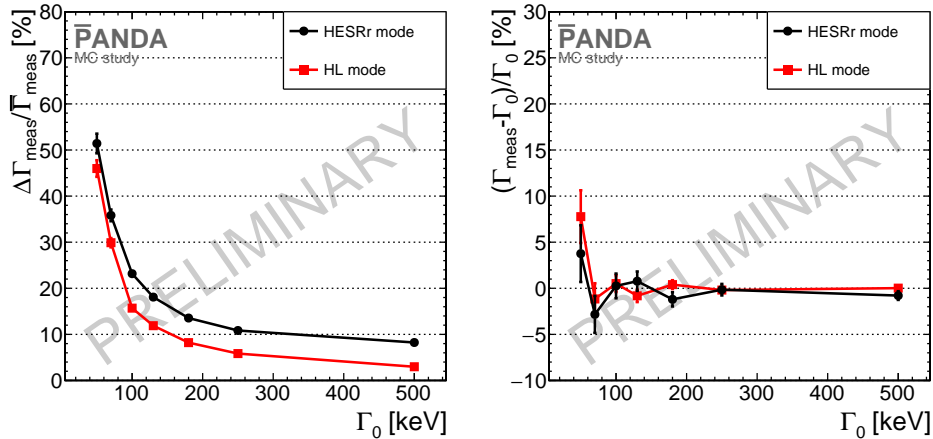


**Figure 2.** The expected sensitivity (left) and bias (right) for the high luminosity mode (red squares) and the high resolution mode (black circles) of HESR.

decuplet predicted the existence of a triple-strange particle with a mass of  $1680 \text{ MeV}/c^2$ . Two years later, the  $\Omega^-$  was discovered which established the Eightfold way [13]. Following it, the quark model was formulated by Gell-Mann and Zweig [14][15].

Today, there are several experiments active in both light and heavy quark baryon spectroscopy. Efforts within light-baryon spectroscopy are mainly focused on  $N^*$  and  $\Delta$  resonances. These resonances have been well studied at various experiments in  $\pi N$  and  $\gamma N$  production channels. In the heavy quark ( $c, b$ ) sector, B-factories (BaBar and Belle) and LCHb have opened up the possibility of studying baryons with charmed and even bottom quarks. Charmed baryons can be produced in B-meson decays at BaBar and Belle and bottomed baryons can be produced in  $Z^0 \rightarrow \bar{b}b$  decays at LHCb. However, the strangeness sector is not as active, which is reflected on scarce data of strange baryons. Currently, there is only one well established excited  $\Xi^*$  resonance and no excited  $\Omega^*$  resonances in the PDG [16].

The prospects of measuring excited multistrange baryons at  $\bar{\text{P}}\text{ANDA}$  have been investigated [17]. The  $\bar{\Xi}^+\Xi^-(1820) + c.c.$ , where  $\Xi^-(1820) \rightarrow \Lambda K^-$  and  $\bar{\Xi}^+ \rightarrow \bar{\Lambda}\pi^+$ , process has been simulated. The decay  $\Xi^-(1820) \rightarrow \Lambda K^-$  was assumed to have a branching ratio of 100%. With a production cross section of  $\sigma(\bar{p}p \rightarrow \bar{\Xi}^+\Xi^-(1820)) \approx 1\mu\text{b}$  and the startup phase luminosity, an event rate of  $15000 \text{ d}^{-1}$  is expected, shown in Table 1.

## 5. Hyperon dynamics

$\bar{\text{P}}\text{ANDA}$  will produce a large amount of antihyperon-hyperon pairs through the reaction  $\bar{p}p \rightarrow \bar{Y}Y$ . In such reactions, the energy scale is given by the mass of the strange quark  $m_s \approx 100 \text{ MeV}/c^2$ , which is below the QCD cut-off  $\Lambda_{\text{QCD}}$  scale. In this energy region, it is unclear what the relevant degrees of freedom are. It could either be quarks and gluons or hadrons. Since perturbation theory is no longer applicable in this regime, alternative phenomenological models are needed. Descriptions of  $\bar{p}p \rightarrow \bar{Y}Y$  have been made in both constituent quark-gluon pictures [18, 19, 20, 21, 22] as well as kaon exchange pictures [18, 23, 24, 25, 26]. There have also been efforts to combine the two approaches [27].

Spin observables are very powerful tools to discriminate between different model predictions. The PS185 collaboration has provided a large sample of single-strangeness hyperons produced in the  $\bar{p}p \rightarrow \bar{Y}Y$  reaction [28]. The measurements of spin observables published by the PS185 collaboration have been decisive in testing different polarization predictions and have sparked

**Table 1.** Expected production rates of hyperons at  $\overline{\text{P}}\text{ANDA}$  with luminosity  $\mathcal{L} = 10^{31} \text{cm}^{-2} \text{s}^{-1}$ . The cross sections  $\sigma(\overline{p}p \rightarrow \overline{\Lambda}\Sigma^0)$  and  $\sigma(\overline{p}p \rightarrow \overline{\Xi}^+\Xi^-)$  are extrapolated values. The cross sections  $\sigma(\overline{p}p \rightarrow \overline{\Omega}^+\Omega^-)$  and  $\sigma(\overline{p}p \rightarrow \overline{\Lambda}_c\Lambda_c)$  are based on theoretical predictions.

$p_{\overline{p}}$ (GeV/c)	Reaction	$\sigma$ ( $\mu\text{b}$ )	Eff (%)	Decay	Rate
1.64	$\overline{p}p \rightarrow \overline{\Lambda}\Lambda$	64	10	$\Lambda \rightarrow p\pi^-$	$28 \text{ s}^{-1}$
4.0	$\overline{p}p \rightarrow \overline{\Lambda}\Sigma^0$	$\sim 40$	30	$\Sigma^0 \rightarrow \gamma$	$30 \text{ s}^{-1}$
4.0	$\overline{p}p \rightarrow \overline{\Xi}^+\Xi^-$	$\sim 2$	20	$\Xi^- \rightarrow \Lambda\pi^-$	$2 \text{ s}^{-1}$
12.0	$\overline{p}p \rightarrow \overline{\Omega}^+\Omega^-$	$\sim 0.002^*$	$\sim 30$	$\Omega^- \rightarrow \Lambda K^-$	$\sim 4 \text{ h}^{-1}$
12.0	$\overline{p}p \rightarrow \overline{\Lambda}_c\Lambda_c$	$\sim 0.1^*$	$\sim 30$	$\Lambda_c \rightarrow \Lambda\pi^+$	$\sim 2 \text{ d}^{-1}$
4.6	$\overline{p}p \rightarrow \overline{\Xi}^+\Xi^-(1820)$	1	5	$\Xi^-(1820) \rightarrow \Lambda K^-$	$15000 \text{ d}^{-1}$

ambitions of measuring and testing spin observables in  $\overline{p}p \rightarrow \overline{Y}Y$  reactions with multi-strange as well as charmed hyperons.

The parity violating weak decay of hyperons means that the spin observables are accessible in the angular distributions of their decay particles. For example, when considering the decay  $\Lambda \rightarrow p\pi^-$ , the  $\Lambda$  polarization manifests in the angular distribution of the decay proton  $I(\cos\theta_p) = \frac{1}{4\pi}(1 + \alpha_\Lambda P_n \cos\theta_p)$ , where  $\alpha_\Lambda = 0.64$  [16] is the decay asymmetry parameter. The polarization is also accessible from hyperons which decay into other hyperons. In the decay  $\Xi^- \rightarrow \Lambda\pi^-$ , where  $\Lambda \rightarrow p\pi^-$ , the polarization as well as the  $\beta$  and  $\gamma$  decay asymmetry parameters are accessible in the joint angular distribution of the  $\Lambda$  hyperon and the proton. Hyperons with spin- $\frac{3}{2}$  such as the  $\Omega^-$  have seven polarization parameters. Three polarization parameters are accessible in the angular distribution of the decay  $\Omega^- \rightarrow \Lambda K^-$ . In the case of the decay  $\Lambda \rightarrow p\pi^-$ , the remaining four polarization parameters are obtained in the joint angular distribution of the  $\Lambda$  hyperon and the proton.

$\overline{\text{P}}\text{ANDA}$  will have an unpolarized beam and unpolarized target. Thus, the polarization and the spin correlation are accessible. Furthermore, with the increased center-of-mass energy achievable, multi-strange as well as single-charmed hyperon-antihyperon pairs can be produced. Monte Carlo studies have been performed to explore the possibilities of measuring spin observables [29, 30, 31]. In Table 1, the expected production rates are given. The rates are calculated assuming a luminosity of  $\mathcal{L} = 10^{31} \text{cm}^{-2} \text{s}^{-1}$ . The cross section of  $\overline{p}p \rightarrow \overline{\Lambda}\Lambda$  is well known. The  $\overline{\Lambda}\Sigma^0$  and  $\overline{\Xi}^+\Xi^-$  cross sections are obtained by extrapolating measurements at other energies. The  $\overline{\Omega}^+\Omega^-$  and  $\overline{\Lambda}_c\Lambda_c$  cross sections are based on theoretical predictions [32, 33, 34, 35, 36]. From the expected rates, the spin observables of single-strange hyperon production can be measured with unprecedented precision during the first year of data taking. Furthermore, the spin observables of double-strange hyperons can be measured for the first time. As more data is accumulated the following years, the polarization parameters of the  $\Omega^-$  hyperon can be measured as well.

## 6. Other physics topics

$\overline{\text{P}}\text{ANDA}$  has a broad physics programme, comprising many topics which were not described in these proceedings. The topics include light meson spectroscopy, open charm physics, structure of nucleons, in-medium properties of hadrons and CP-violation studies. The modular design of  $\overline{\text{P}}\text{ANDA}$  also opens up the possibility to produce and study hypernuclei.

## 7. Summary

During the first year of operation, the spin observables in single-strange hyperon production in  $\bar{p}p \rightarrow \bar{Y}Y$  processes will be measured with higher statistical precision and for the first time, spin observables of double-strange hyperon production will be measured. Furthermore, the full spectrum of single- and double-strange excited hyperons can be measured with unprecedented statistical precision. As the facility matures and more data is collected, the polarization parameters of the  $\Omega^-$  can be measured for the first time and the full triple-strange excited hyperon spectrum will be accessible. By producing the  $X(3872)$  in direct formation, an energy scan of its line-shape can be performed which will allow to distinguish between the different theoretical interpretations of its nature. With 80 days of beam time, such a measurement is sensitive to widths an order of magnitude smaller than the current upper limit for the width of the  $X(3872)$ .

## References

- [1] Kotulla M *et al.* PANDA Collaboration 2005 *PANDA Technical Progress Report*
- [2] Choi S-K *et al.* Belle Collaboration 2003 *Phys. Rev. Lett.* **91**, 262001
- [3] Auber B *et al.* Babar Collaboration 2005 *Phys. Rev. D* **71** 071103
- [4] Acosta D *et al.* CDF II Collaboration 2004 *Phys. Rev. Lett.* **93** 072001
- [5] Abazov V M *et al.* D0 Collaboration 2004 *Phys. Rev. Lett.* **93** 162002
- [6] Aaij R *et al.* LHCb Collaboration 2012 *Eur. Phys. J. C* **72** 1972
- [7] Chatrchyan S, Khachatryan V *et al.* CMS collaboration 2013 *J. High Energy. Phys.* **1304** 154
- [8] Aaij R *et al.* LHCb Collaboration 2013 *Phys. Rev. Lett.* **110** 222001
- [9] Hanhart C *et al.* 2007 *Phys. Rev. D* **76** 034007
- [10] Braaten E and Lu M 2008 *Phys. Rev. D* **77**, 014029
- [11] Choi S-K *et al.* Belle Collaboration 2011 *Phys. Rev. D* **84** 052004
- [12] Nerling F 2016 *Talk at the 11th International Workshop on Heavy Quarkonium*
- [13] Barnes V E *et al.* 1964 *Phys. Rev. Lett.* **12** 204
- [14] Gell-Mann M 1964 *A Schematic Model of Baryons and Mesons Phys. Lett.* **8** 214
- [15] Zweig G 1964 *An SU(3) model for strong interaction symmetry and its breaking. Version 1* CERN-TH-401
- [16] K A Olive *et al.* 2014 *Particle Data Group Chin. Phys. C* **38** 090001.
- [17] Pütz J 2016 *Proceedings of FAIRNESS 2016* Garmisch-Partenkirchen, Germany
- [18] Kohno M and Weise W 1986 *Phys. Lett. B* **179** 15
- [19] Rubinstein H R and Snellman H 1985 *Phys. Lett. B* **165** 187
- [20] Furai S and Faessler A 1987 *Nucl. Phys. A* **468** 669
- [21] Burkardt M and Dillig M 1988 *Phys. Rev. C* **37** 1362
- [22] Alber G *et al.* 1988 *Z. Phys. A* **331** 207
- [23] Tabakin F and Eisenstein R A *Phys. Rev. C* **31**, 1857 (1985)
- [24] La France P *et al.* 1988 *Phys. Lett. B* **214** 317
- [25] Timmermans R G E *et al.* 1992 *Phys. Rev. D* **45** 2288
- [26] Haidenbauer J *et al.* 1992 *Phys. Rev. C* **46** 2516
- [27] Ortega P G *et al.* 2011 *Phys. Lett. B* **696** 352
- [28] Johansson T 2003 *Proceedings of 8th Int. Conf. on Low Energy Antiproton Physics* 95
- [29] Erni W *et al.* 2009 PANDA collaboration *Physics Performance Report* arXiv: 0903.3905 [hep-ex]
- [30] Thomé E 2012 *Multi-Strange and Charmed Antihyperon-Hyperon Physics for PANDA* (Ph. D. Thesis, Uppsala University)
- [31] Grape S 2009 *Studies of PWO Crystals and Simulations of the  $\bar{p}p \rightarrow \bar{\Lambda}\Lambda, \bar{\Lambda}\Sigma^0$  Reactions for the PANDA experiment* (Ph.D. Thesis, Uppsala University)
- [32] Kaidalov A B and Volkovitsky P E Z 1994 *Phys. C* **63** 51
- [33] Titov A I and Kampfer B 2008 *Phys. Rev. C* **78** 025201
- [34] Gornitschnig A T *et al.* 2009 *Eur. Phys. J. A* **42** 43
- [35] He J *et al.* 2011 *Phys. Rev. D* **84** 114010
- [36] Khodjamirian A *et al.* 2012 *Eur. Phys. J. A* **48** 31